Molecular Immunology 106 (2019) 143–152

Contents lists available at ScienceDirect

Molecular Immunology

journal homepage: www.elsevier.com/locate/molimm

Electroacupuncture at ST-36 ameliorates DSS-induced acute colitis via regulating macrophage polarization induced by suppressing NLRP3/IL-1β and promoting Nrf2/HO-1

Shuangning Song, Jing An, Yingli Li, Shi Liu*

Department of Gastroenterology, Union Hospital, Tongji Medical College, Huazhong University of Science and Technology, Wuhan, 430022, China

ARTICLE INFO

Keywords:
Electroacupuncture
Colitis
Macrophages
Polarization

ABSTRACT

Background: Electroacupuncture (EA) at ST-36 can attenuate acute experimental colitis, but the mechanisms are unclear. We investigated the role of macrophages in the anti-inflammatory effects of EA and its molecular mechanisms.

Methods: Male C57BL/6 mice were randomized into five groups: normal control, dextran sulfate sodium (DSS)-induced acute colitis (DSS), DSS with sham EA (SEA), DSS with high-frequency EA (HEA) and DSS with low-frequency EA (LEA). Body weight, colon length, DAI score and histological score were evaluated during colitis progression. Serum and colonic levels of pro- and anti-inflammatory cytokines were detected with ELISA, cytometric beads array, RT-PCR and western blotting analysis. Colonic macrophage subsets were determined using flow cytometry. Magnetic-activated cell sorting was applied to isolate colonic macrophages, and molecular mechanisms were explored with western blotting, RT-PCR and immunofluorescence.

Results: (1) Compared with the DSS group, HEA and LEA attenuated body weight loss and decreased DAI and histological scores. (2) Serum levels and colonic protein and mRNA levels of IL-1β, TNFα, IL-6, IL-12 and IL17 were markedly decreased with HEA and LEA. IL-10 level was increased with HEA. (3) M1 macrophage percentage increased, while M2 macrophage percentage decreased in the DSS group; HEA and LEA reversed these proportions. (4) NLRP3/IL-1β protein and mRNA levels in isolated macrophages decreased with HEA and LEA compared with the DSS treatment group; (5) HEA increased Nrf2/HO-1 levels compared with levels in DSS mice.

Conclusion: The anti-inflammatory effects of EA on DSS-induced acute colitis may rely on regulating macrophage polarization, NLRP3/IL-1β suppression and Nrf2/HO-1 promotion.

1. Introduction

Ulcerative colitis (UC) is a chronic disease that is characterized by diffuse inflammation of the rectal and colonic mucosa. The classic clinical symptom is bloody diarrhoea, which is characterized by periods of remission and exacerbation. In contrast to its incidence in developed countries in North America and Eastern Europe, the incidence of UC is increasing in developing nations, including China, over recent decades (Ng et al., 2013; Yang et al., 2014; Zhao et al., 2013). To date, various drugs have been recruited to treat UC. Traditional salazosulfapyridine, glucocorticoids and new immunosuppressive agents are effective, but their side effects and high costs are also unneglectable. In recent years, a few studies have indicated that electroacupuncture (EA) could ameliorate acute experimental colitis (Goes et al., 2014; Jin et al., 2017; Sun et al., 2017; Wu et al., 2007), but the mechanisms underlying this effect were uncertain. Therefore, the specific effects of EA on colitis and the underlying mechanisms need further investigation.

The precise pathogenesis of UC is not fully understood. Aberrant innate and/or adaptive immune responses contribute to the development of UC (Geremia et al., 2014; Shouval et al., 2014), these responses manifests as a burst of pro-inflammatory cytokines, such as IL-1β, TNFα, IL-6, IL-12 and IL17, and inhibition of the anti-inflammatory cytokine IL-10. Of all the inflammatory cells participating in the secretion of these cytokines, especially during the acute phase colitis,

Abbreviations: UC, ulcerative colitis; Nrf2, NFE-related factor 2; HO-1, heme oxygenase-1; DAI, disease activity index; MACS, magnetic-activated cell sorting; H&E, haematoxylin and eosin; PE, phycoerythrin; GAPDH, glyceraldehyde-3-phosphate dehydrogenase; RIPA, radioimmunoprecipitation; BCA, bicinchoninic acid; SDS–PAGE, sodium dodecyl sulfate polyacrylamide gel electrophoresis; ECL, enhanced chemiluminescence; ANOVA, analysis of variance; DNBS, dinitrobenzene sulfonic acid; CD, Crohn's disease

* Corresponding author at: No.1277, Jiefang Road, Wuhan Union Hospital, Wuhan, Hubei Province, 430022, China.
E-mail address: shiliugao@yahoo.com (S. Liu).

https://doi.org/10.1016/j.molimm.2018.12.023
Received 18 July 2018; Received in revised form 5 December 2018; Accepted 21 December 2018
Available online 02 January 2019
0161-5890/

macrophages are the most abundant and crucial (Gren and Grip, 2016). Activated macrophages can be functionally divided into classically activated (M1 type) and alternatively activated (M2 type) cells in response to different stimuli, and these different types play opposite roles in the development of UC (Isidro and Appleyard, 2016). M1 macrophages secrete pro-inflammatory cytokines, causing mucosal damage. In contrast, M2 macrophages express high levels IL-10, promoting mucosal repair (Hunter et al., 2010). However, it is unknown whether EA can regulate macrophage polarization in UC.

Studies on the molecular mechanisms of macrophages in regulating inflammation have been striking in recent years. In vitro studies have shown that macrophage lines are activated to secrete IL-1β through the activation of NLRP3 in mice with dextran sulfate sodium (DSS)-induced colitis (Bauer et al., 2010). Moreover, it has been demonstrated in vivo that experimental colitis can be ameliorated by suppressing NLRP3 activation in colonic macrophages (Simovic Markovic et al., 2016). In contrast, the pro-inflammatory effect of LPS-stimulated macrophages was inhibited by enhancing the NFE-related factor 2 (Nrf2) pathway (Liu et al., 2016; Wang et al., 2016). Nrf2 plays a key role in the antioxidant response by directing transcription of the antioxidant enzyme heme oxygenase-1 (HO-1), and HO-1 can modulate IL-10 production (Kim et al., 2010; Naito et al., 2014). Therefore, whether EA could regulate macrophages through the abovementioned mechanisms requires a more thorough exploration.

In the present study, we aim to clarify the effects of different frequencies of EA on acute colitis induced by DSS and to further explore whether macrophage polarization and potential molecular signalling (NLRP3/IL-1β and Nrf2/HO-1) are involved in EA-induced amelioration of acute colitis.

2. Materials and methods

2.1. Animals

Eighty male C57BL/6 mice, six to eight weeks of age, were used in this study. These mice were purchased from Beijing Hua Fu Kang Biotechnology Co, LTD, Beijing, China. They were housed in standard conditions (22 °C, 12 h/12 h light-dark cycle) and given free access to food and drink. All animals were adapted to the environment for two weeks before entering the formal study. This study was carried out in accordance with the principles of the Guide for the Care and Use of Laboratory Animals of Tongji Medical College, the Committee of Experimental Animals of Tongji Medical College of Huazhong University of Science and Technology.

2.2. Experimental protocols

All of the mice were randomly divided into five groups: the control group (n = 16), the group of mice with DSS-induced colitis (DSS, n = 16), the group of mice with DSS-induced colitis treated with sham EA (SEA, only acupuncture without electric current, n = 16), the group of mice with DSS-induced colitis treated with high-frequency EA (HEA,100 Hz, 1 mA, n = 16), and the group of mice with DSS-induced colitis treated with low-frequency EA (LEA, 10 Hz, 1 mA, n = 16). The experimental period was seven days, from day 0 to day 6. All groups, except for the control group, were given 2.5% DSS (36000–50000 MW; MP Biomedical, Solon, OH, USA) in their drinking water from day 1 to day 6. The control group mice were given plain water. EA at acupoint ST-36 was applied to the SEA, HEA and LEA groups from day 1 to day 6. Body weight, stool consistency and rectal bleeding were observed daily. At day 6, all mice were sacrificed after getting blood from the heart. Colon specimens were carefully obtained, and colon length was measured. The disease activity index (DAI) was calculated as the combined scores for weight loss (0–4), stool consistency (0–4) and bleeding (0, 2, 4), as previously described (Bang and Lichtenberger, 2016). The colon tissues of some mice were immediately used for flow cytometry and magnetic-activated cell sorting (MACS). The other tissues were stored at −80 °C.

2.3. EA

The method applied was almost the same as described previously (Tian et al., 2017). Briefly, the acupoint ST-36 was selected, which is located on the posterolateral side of the knees approximately 2 mm below the fibular head; EA was applied to both hind limbs. For the groups actually treated with EA, a pair of stainless steel needles (0.16 × 7 mm) were inserted at a depth of 2–3 mm at the bilateral acupoints of the hind limbs. The electrical current was increased until the bilateral hind limbs started to tremble slightly, and stimulation was sustained for as long as 30 min. The sham group underwent the same procedure as groups actually treated with EA but without an electrical current.

2.4. Histological analysis

The colonic tissues of six mice from each group were fixed with 4% paraformaldehyde and embedded with paraffin. Then, the paraffin sections of each colon were stained with haematoxylin and eosin (H&E). The histological scores were calculated based on the scoring criteria for DSS-induced colitis as described previously (Wirtz et al., 2007); scores ranged from 0 to 4.

2.5. Serum cytokines analysis by enzyme-linked immunosorbent assay (ELISA) and cytometric beads array (CBA)

Serum from six to eight mice for each group were used to perform ELISA and CBA analyses. The amount of IL-1β in serum was quantified using an ELISA kit (Abclonal, Wuhan, China) according to the manufacturer's instruction. The levels of TNFα, IL-6, IL-12 and IL-10 were detected by CBA assay (BD Biosciences, New Jersey, USA). Briefly, standard protein samples were serially diluted, and then, microparticles were prepared and mixed with the serum. Phycoerythrin (PE)-conjugated antibodies against these cytokines were added, and the mixtures were incubated for 3 h in the dark at room temperature. The mixtures were washed and centrifuged at 1000 rpm for 5 min, and the pellets were resuspended in 200 μl wash buffer. A BD LSR Fortessa X-20 system was calibrated with setup beads, and 3000 events were acquired for each sample. Individual cytokine concentrations were calculated based on the standard curve and their fluorescence intensities.

2.6. Isolation of colonic lamina propria mononuclear cells (LPMCs)

Tissues of eight mice from each group were used for the isolation of colonic LPMCs. As described previously (Weigmann et al., 2007), the colon tissues were placed in a pre-digestion solution [1 × Hank's balanced salt solution (HBSS) containing 5 mM EDTA (Sigma-Aldrich) and 1 mM DTT (Roche)] at 37 °C with shaking for 20 min twice to remove epithelial cells. After being filtered with a 100-μm cell strainer, the remaining pieces were then digested with digestion solution [1 × phosphate-buffered saline (PBS) containing 0.05% collagenase D (Roche), 0.05% DNase I (Sigma-Aldrich) and 0.3% Dispase II (Sigma-Aldrich)] at 37 °C for 1 h. The suspensions were then passed through 40-μm cell strainer and centrifuged for 10 min at 500 × *g* at room temperature. The cells were harvest and resuspended in 4 ml PBS, and then, the cell suspension was placed on the top of the same volume of Ficoll solution in a 10 ml glass tube. Samples were the centrifuged continuously at 2400 rpm at 20 °C for 20 min. Then, LPMCs were carefully collected in new tubes for subsequent flow cytometry analysis or MACS.

2.7. Flow cytometry analysis of LPMCs

The colonic LPMCs of four mice from each group were selected for

flow cytometry analysis. Briefly, after cell counting, the LPMCs were incubated with anti-mouse F4/80 conjugated with PE (BD biosciences, New Jersey, USA), anti-mouse CD16/32 conjugated with PerCP/Cy5.5 (BD biosciences, New Jersey, USA), and anti-mouse CD206 conjugated with Alexa 647 (BD biosciences, New Jersey, USA) for 1 hat room temperature. The cells were washed twice with PBS and then assessed by flow cytometry using a BD LSR Fortessa X-20 system. The data were analysed by FlowJo V10 software.

2.8. MACS

The remaining four colonic LPMCs from each group were used for magnetic cell sorting. After determining the number of LPMCs, the cell suspension was centrifuged at 300 × *g* for 10 min, and the supernatant was completely aspirated. Then, the cell pellet was resuspended in 90 µl of buffer per 10^7 cells. Next, 10 µl of Anti-F4/80 MicroBeads UltraPure (Miltenyi Biotec, Bergisch Gladbach, Germany) per 10^7 cells was added, and samples were incubated for 15 min in the dark in the refrigerator (2–8 °C). After washing the cells and centrifuging them as described above, the supernatants were aspirated and resuspended at up to 10^8 cells in 500 µl of buffer. Finally, magnetic separation of F4/80 macrophages with MS columns (Miltenyi Biotec, Bergisch Gladbach, Germany) was performed according to the manufacturer's instructions.

2.9. RNA extraction and quantitative real-time PCR (RT-PCR) analysis

The total RNA of the separated macrophages and colonic tissues (from eight mice in each group) were isolated using TRIzol reagent (Takara, Otsu, Japan), and then, cDNA was synthesized using Prime Script™ RT Master Mix (Perfect Real-Time; Takara, Otsu, Japan) according to the instructions. The internal control was glyceraldehyde-3-phosphate dehydrogenase (GAPDH). RT-PCR was performed using the SYBR-Green PCR master mix. All reactions were performed in duplicate in a 10 µl volume containing 1 µl cDNA, 5 µl SYBR-Green reaction mix (Takara, Otsu, Japan), 0.5 µl sense primer, 0.5 µl antisense primer (both from Invitrogen), and 3 µl ddH2O. All reactions were performed in a Roche LightCycler R480 (Roche, Switzerland). Relative changes in gene expression were determined using the 2 –ΔCt method (ΔCt = CT target-CT GAPDH). The primer sequences were as follows:

IL-1β forward, 5′-GGAGAGCCCTGGATACCAAC-3′
reverse, 5′-CAGGGTCCCAGACAGAAGTT-3′;
TNFα forward, 5′-CTTGGAAATAGCTCCCAGAA-3′ and
reverse, 5′-CATTTGGGAACTTCTCATCC-3′;
IL-6 forward, 5′ − CCGGAGAGGAGACTTCACAG-3′and
reverse, 5′-CAGAATTGCCATTGCACAAC– 3′;
IL-12 forward, 5′-GCCGGCTATCCAGACAATTA-3′and
reverse, 5′-GGCCAAACTGAGGTGGTTTA-3′;
IL-10 forward, 5′-TGCTATGCTGCCTGCTCTTA-3′ and
reverse, 5′-TCATTTCCGATAAGGCTTGG-3′;
IL-17 forward, 5′-CTCCAGAAGGCC CTCAGACTAC-3′ and
reverse, 5′-GCTTTCCCTCCGCATTGACACAG-3′;
iNOS forward, 5′-CAGCTGGGCTGTACAAACCTT-3′ and
reverse, 5′-CAGCTGGGCTGTACAAACCTT-3′;
CD206 forward, 5′-CAGGTGTGGGCTCAGGTAGT-3′ and
reverse, 5′-TGTGGTGAGCTGAAAGGTGA-3′;
Arg-1 forward, 5′-TTGGGTGGATGCTCACACTG-3′ and
reverse, 5′-TTGCCCATGCAGATTCCC-3′;
FIZZ1 forward, 5′-TCCCAGTGAATACTGATGAGA-3′ and
reverse, 5′ − CCACTCTGGATCTCCCAAGA-3′;
NLRP3 forward, 5′- AGAAGAGACCACGGCAGAAG-3′ and
reverse, 5′ − CCTTGGACCAGGTTCAGTGT- 3′;
Nrf2 forward, 5′-GGGATGAGCTAGTGCTGATCTGG-3′ and
reverse, 5′-AAACTTGCTCCATGTCCTGCTCTA-3′;
HO-1 forward, 5′-TGCAGGTGATGCTGACAGAGG-3′ and
reverse, 5′-GGGATGAGCTAGTGCTGATCTGG-3′;
GAPDH forward, 5′-GCATTGTGGAAGGGCTCATG-3′ and
reverse, 5′-TTGCTGTTGAAGTCGCAGGAG-3′.

2.10. Western blotting analysis

The isolated macrophages and colonic tissues of eight mice from each group were used for western blotting analysis. The macrophage lysates and the frozen colonic samples were homogenized in radioimmunoprecipitation assay (RIPA) buffer supplemented with a protease inhibitor. Then, samples were incubated on ice for 30 min and centrifuged at 12,000 rpm at 4 °C for 15 min. The supernatant included the total protein content and was added to the loading buffer for subsequent protein degeneration. A bicinchoninic acid (BCA) protein assay kit was employed to measure protein concentration. Denatured protein samples of appropriate quality were loaded onto sodium dodecyl sulfate polyacrylamide gel electrophoresis (SDS–PAGE) gels and, following separation, transferred to PVDF membranes. Membranes werethen blocked with 5% nonfat dry milk in Tris-buffered saline containing 0.1% Tween 20 (TBST) for 1 h at room temperature. Next, membranes were incubated with the following primary antibodies: goat anti-IL-1β (1:1000, R&D Systems, Minneapolis, USA), goat-anti TNFα (1:2000, R&D Systems, Minneapolis, USA), rat anti-IL-6 (1:500, R&D Systems, Minneapolis, USA), goat-anti- IL-12 (1:2000, R&D Systems, Minneapolis, USA), rat anti-IL-10 (1:500, R&D Systems, Minneapolis, USA), rabbit anti-IL17 (1:200, Abclonal, Wuhan, China), rat anti-NLRP3 (1:200, R&D Systems, Minneapolis, USA), mouse anti-IL1β (1:1000, Cell signalling Technology, Massachusetts, USA), rabbit anti cleaved IL1β (1:1000, Cell signalling Technology, Massachusetts, USA), Mouse anti-caspase1(1:200, Santa Cruz, California, USA), rabbit anti cleaved caspase1 (1:1000, Cell signalling Technology, Massachusetts, USA), rabbit anti-Nrf2 (1:500, Proteintech, Wuhan, China), and rabbit anti HO-1 (1:100000, Abcam, Cambridge, MA, USA) overnight at 4 °C, with rabbit anti-mouse GAPDH (1:5000, Abbkine, Inc., Redlands, CA, USA) serving as the internal control. Then, membranes were washed three times for 5 min each with TBST and incubated with horse radish peroxidase (HRP)-linked rabbit anti goat IgG, HRP-linked rabbit anti rat IgG, and HRP-linked goat anti-rabbit IgG (1:4000, Antgene, Wuhan, China) for 1 h at room temperature. After 3 additional washes with TBST, the protein bands were detected using an enhanced chemiluminescence (ECL) agent (ThermoFisher, USA). Densitometry analysis was performed with Quantity One software (Bio-Rad Technical Service Department, Version 4.6.2).

2.11. Immunofluorescence staining

Paraffin-embedded colonic sections (from six mice in each group) were dewaxed with dimethyl-benzene and hydrated in a graded alcohol series. Then, antigens were retreved under high pressure. The sections were blocked with 5% donkey serum. Sections were then incubated with primary antibodies (rat-anti F4/80, 1:100, Abcam, Cambridge, MA, USA; goat-anti NLRP3, 1:50, Abcam, Cambridge, MA, USA; rabbit anti HO-1, 1:200, Abcam, Cambridge, MA, USA) diluted in 1% donkey serum at 4 °C overnight. After washing the sections three times with PBST, sections were incubated with secondary antibodies (Daylight 594-conjugated donkey anti-rat IgG, 1:200, Abbkine; Daylight 488-conjugated donkey anti-rabbit IgG, 1:200, Abbkine; Daylight 488 with donkey anti-goat IgG, 1:200, Abbkine) diluted in PBST for 1 h at room temperature. Sections were washed three times as above, and nuclei were stained with DAPI for 10 min at room temperature. Finally, the sections were sealed with anti-fluorescence quenching sealant. A confocal microscope (Olympus, Tokyo, Japan) was used to examine the sections. The mean optical density (MOD) was analyzed by Imageproplus 6.0 software.

2.12. Statistical analysis

All data are expressed as the means ± SEM. Analysis of variance

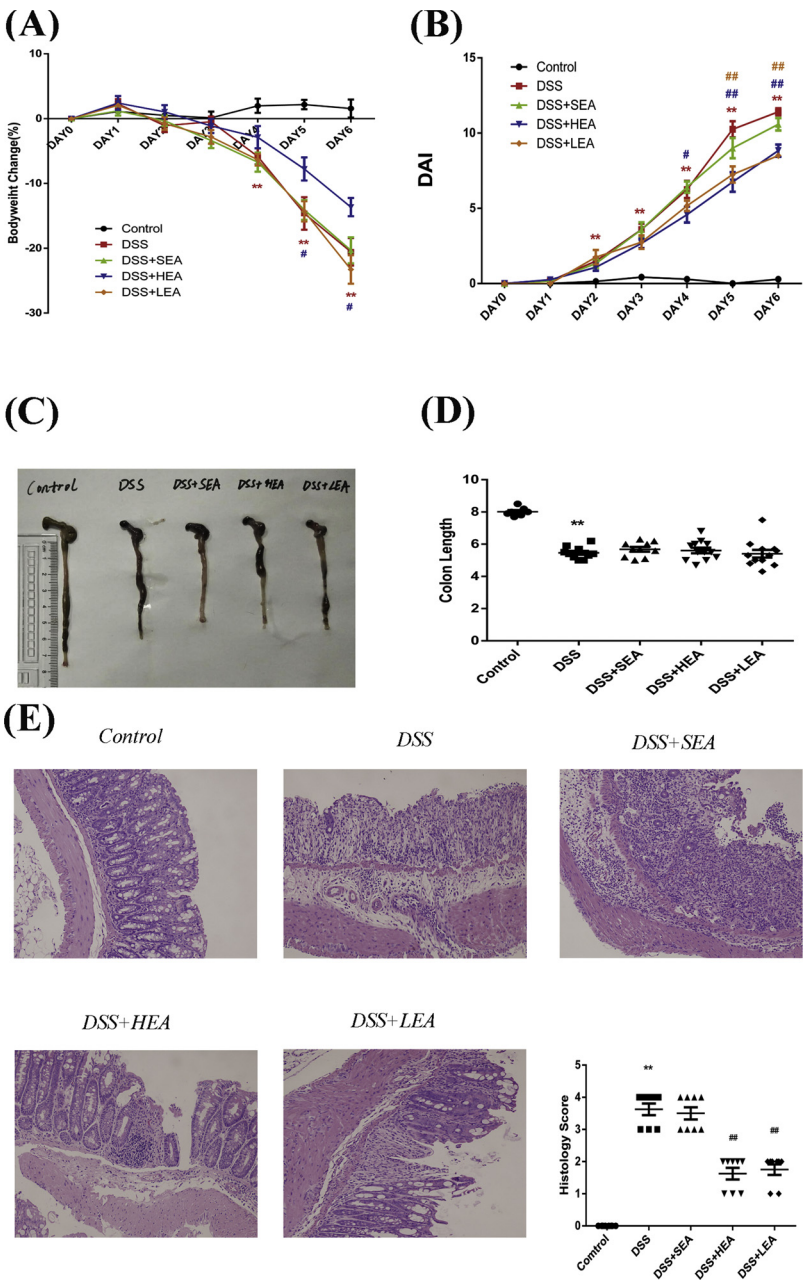

Fig. 1. Colonic inflammation was ameliorated in the EA-treated mice following DSS exposure. (**A**) Bodyweight change were measured every day and are expressed as the percentage change from day 0; n = 16 in each group. (**B**) Clinical DAI scores from each group were assessed every day; n = 16 in each group. (**C, D**)The lengths of colons from each group were measured; n = 16 in each group. (*E*) H&E staining was performed, and histological scores were determined; n = 6 in each group. Representative photomicrographs of colon sections stained with H&E were examined at 400× magnification. $^{*}P < 0.05$ compared with the control group, $^{**}P < 0.01$ compared with the control group, $^{\#}P < 0.05$compared with the DSS group and $^{\#\#}P < 0.01$compared with the DSS group. DAI, disease activity index; DSS, dextran sulfate sodium; H&E, haematoxylin and eosin.

(ANOVA) were used to compare the differences among different groups. P values less than 0.05 indicated a statistically significant difference. The statistical analysis was performed using SPSS 21.0 (SPSS Inc., Chicago, IL)

3. Results

3.1. EA ameliorates DSS-induced acute colitis

In our experiment, we observed changes in bodyweight, colon length and DAI scores to assess the severity of symptoms (Fig. 1a–d). DSS exposure induced significantly greater weight loss from day4 throughout the experiment (P = 0.001). Moreover, the DAI of the DSS group was obviously increased from day2 compared with that of the controls (P < 0.001). Meanwhile, a greater shorting of colon length was discovered at the end of the experiment in the DSS group compared with the length in the controls (P < 0.001). Notably, compared with weight loss in the DSS group, we observed an attenuation of weight loss with HEA treatment atday5 and day6 (P = 0.019 and P = 0.027, respectively); both HEA and LEA decreased the DAI score at day5 and day6 (all P < 0.01). No effect was found with the SEA treatment regarding weigh change, DAI score or colon length (all P > 0.05). As shown in Fig. 1e, compared with the control group, DSS exposure induced severe mucosal damage, with transmural leukocyte infiltration. Consistent with the remarkable amelioration in clinical signs, the HEA and LEA mice showed low-level or moderate inflammation, with scattered infiltrating immune cells and multiple foci. The results were further confirmed by histological scoring. Scores were higher in the DSS group than in the controls (P < 0.001) and were decreased with HEA and LEA treatment (both P < 0.001)

3.2. EA maintains a balance of the secretion of pro-inflammatory and anti-inflammatory cytokines in DSS-induced colitis

Then, we measured the concentration of pro-inflammatory cytokines IL-1β, TNFα, IL-6 and IL-12 in the serum by ELISA and CBA. As

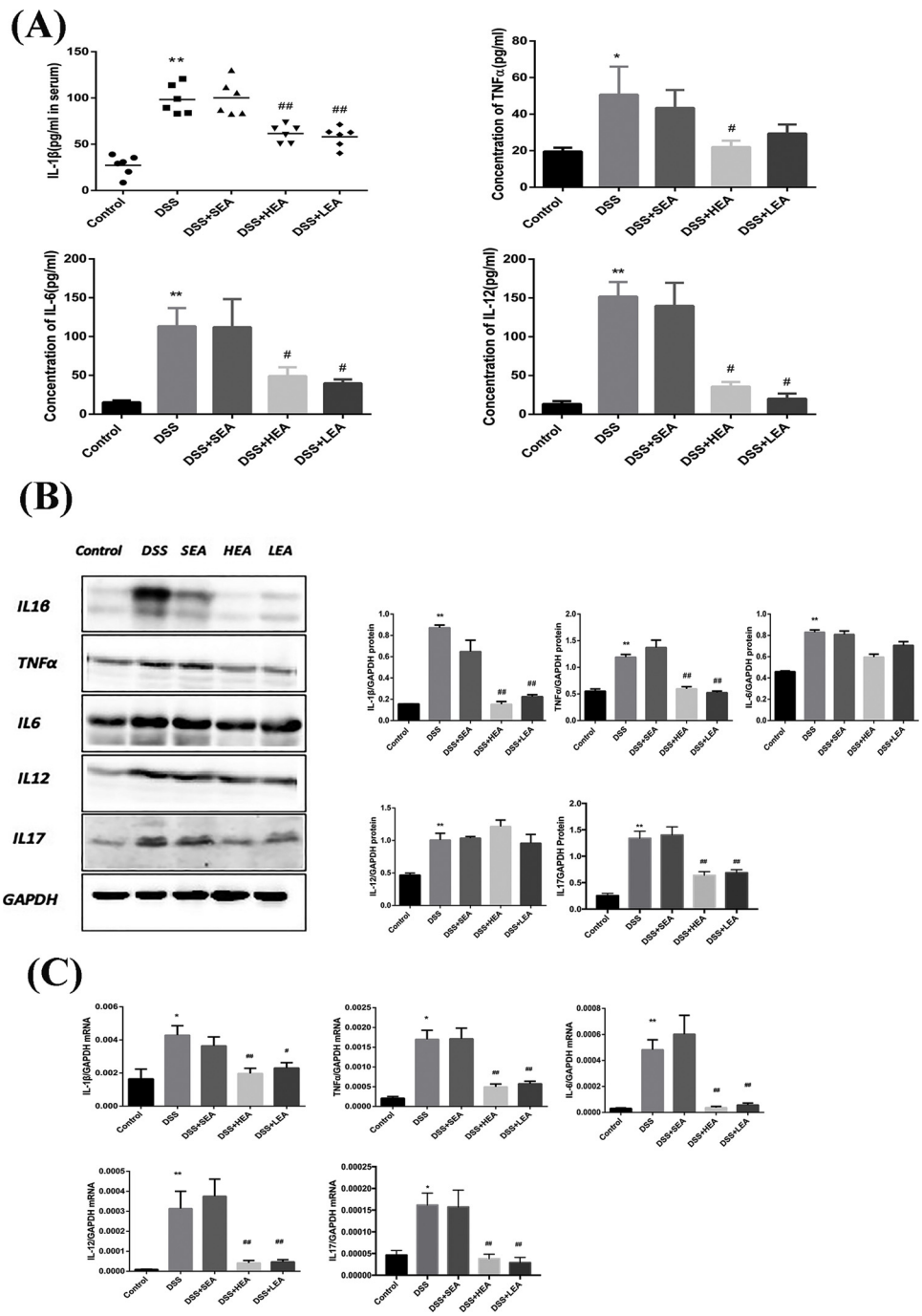

Fig. 2. Decreased serum and colon levels of pro-inflammatory cytokines in EA-treated mice following DSS exposure. (**A**) The serum level of IL-1β was measured by ELISA, n = 6 in each group; and the levels of cytokines (TNFα, IL-6 and IL-12) were measured by CBA, n = 8 in each group. (**B**) The protein levels of IL-1β, TNFα, IL-6, IL-12 and IL17 in the colon were measured by western blotting; n = 8 in each group. (**C**) The mRNA expression of IL-1β, TNFα, IL-6, IL-12 and IL17 in the colon were examined by RT-PCR analysis; n = 8 in each group. $^{*}P < 0.05$ compared with the control group, $^{**}P < 0.01$ compared with the control group, $^{\#}P < 0.05$compared with the DSS group and $^{\#\#}P < 0.01$compared with the DSS group. CBA, cytometric beadarray; ELISA, enzyme-linked immunosorbent assay.

shown in Fig. 2a, secretion of IL-1β, TNFα, IL-6 and IL-12 was greater in the DSS group than in the controls (for TNFα P = 0.047, all others $P < 0.01$). Both HEA and LEA decreased the levels of IL-1β, IL-6 and IL-12 (for IL-1β $P < 0.001$, all others $P < 0.05$). The serum level of TNFα was decreased only with the HEA treatment (P = 0.044). No differences in the secretion of these cytokines were found between the DSS and SEA groups (all $P > 0.05$). Moreover, a western blotting analysis was used to further measure pro-inflammatory cytokines protein expression in colonic tissues. They were obviously upregulated in mice in the DSS group compared with control group (all $P < 0.01$). In the HEA and LEA groups, the protein levels of IL-1β, TNFα and IL17 were dramatically decreased compared with expression in the DSS group (all $P < 0.01$) (Fig. 2b). The mRNA expression of IL-1β, TNFα, IL-6, IL-12 and IL17 were all decreased by both HEA and LEA treatment compared with expression in the DSS group (all $P < 0.01$) (Fig. 2c).

The serum concentration of anti-inflammatory cytokine IL-10 was also measured with CBA. As demonstrated in Fig. 3a, serum levels of IL-10 were remarkably promoted with HEA treatment (P = 0.011). Meanwhile, as shown by western blotting analysis, colonic protein levels of IL-10 in the DSS group were increased compared to levels the controls ($P < 0.001$). However, levels were even higher in the HEA group than in the DSS group (P = 0.008). In addition, both HEA and LEA stimulated the mRNA expression of IL-10 in colonic tissue ($P < 0.029$ and P = 0.011, respectively) (Fig. 3b).

3.3. EA suppressed M1 macrophage polarization and promoted M2 macrophage polarization

We next investigated the effect of EA on macrophage polarization. Colonic LPMCs were isolated and analysed with flow cytometry. F4/

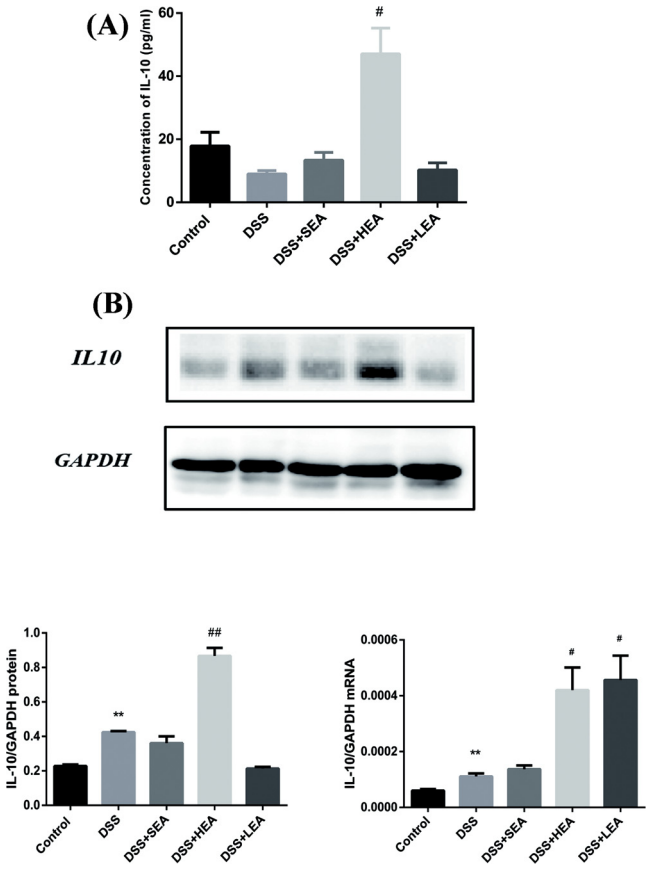

Fig. 3. Increased serum and colon levels of the anti-inflammatory cytokine IL-10 in EA-treated mice following DSS exposure. (**A**) The serum levels of IL-10 were measured by CBA, n = 8 in each group. (**B**) The protein and mRNA levels of IL-10 inthe colon were measured by western blotting and RT-PCR, n = 8 in each group. $^{**}P < 0.01$ compared with the control group, $^{\#}P < 0.05$compared with the DSS group and $^{\#\#}P < 0.01$compared with the DSS group.

80^+ cells were considered to represent all macrophages, $F4/80^+CD16/32^+$cells were considered M1 macrophages, and $F480^+CD16/32^-CD206^+$cells were considered M2 macrophages. As depicted in Fig. 4a, we found that the percentage of $F4/80^+$ macrophages was increased ($P < 0.001$); meanwhile, the proportion of M1 macrophages was increased ($P < 0.001$) and the proportion of M2 macrophages was decreased ($P = 0.008$) in the DSS group compared with proportions in the controls. Furthermore, compared with the DSS group, both the HEA and LEA groups showed decreased percentages of M1 macrophages, from above 80% to under 60%, and increases in the percent of M2 macrophages, from less than 1% to almost 5% (all $P < 0.01$). SEA treatment did not change the proportions of M1 macrophages or M2 macrophages. ($P = 0.930$ and $P = 0.997$, respectively).

Then, we isolated the F4/80+ macrophages by MACS and further examined the mRNA expression levels of M1 and M2 macrophage-associated genes with RT-PCR (Fig. 4b). DSS exposure increased the mRNA expression of iNOS, CD206 and FIZZ1 (all $P < 0.01$). Notably, the expression of the M1-associated gene iNOS was significantly decreased in HEA- and LEA-treated mice compared with expression in the DSS group ($P = 0.007$ and $P = 0.009$, respectively). In contrast, expression of the M2-associated gene Arg1 was increased by both HEA and LEA treatment ($P = 0.011$ and $P = 0.017$, respectively). Moreover, the expression of CD206 was promoted by HEA ($P = 0.003$), and FIZZ1 expression was increased only by LEA ($P = 0.012$).

3.4. EA inhibited NLRP3/IL-1β activation and promoted Nrf2/HO-1 activation in macrophages

Finally, we explored the effect of EA on NLRP3/IL1β signalling pathwany by western blotting (Fig. 5a). As expected, the NLRP3 inflammasome was dramatically activated, followed by caspase1 activation in the DSS group compared with the control group ($P = 0.004$ and $P = 0.036$, respectively). In addition, the level of cleaved IL1β was significantly increased in the DSS mice ($P = 0.001$). Both the HEA and LEA treatment supressed the activation of NLRP3 and caspase1, the cleavage of IL1β was also reduced (all $P < 0.05$); no similar effect was obtained with SEA treatment (all $P > 0.5$). We then investigated the effect of EA on the activation of Nrf2/HO-1. In the DSS group, protein levels of Nrf2 were decreased ($P = 0.013$). Only HEA treatment effectively promoted the protein levels of Nrf2 ($P < 0.001$) and HO-1 ($P = 0.002$) compared with the levels in the DSS group. An analogous situation was found for mRNA expression (Fig. 5b).

Immunofluorescence double staining co-localization was used to further investigate NLRP3 activation and HO-1 expression in the macrophages (Fig. 6). In the control group, there was minimal expression of F4/80 and NLRP3 in the integrated mucosa. However, the structure of the mucosa was disrupted in the DSS group, which was accompanied by increased F4/80 and NLRP3 co-localization ($P = 0.002$). With HEA and LEA treatment, we found that NLRP3 expression in F4/80-positive areas was decreased ($P = 0.003$, $P = 0.03$). There was no difference between the DSS group and SEA group ($P = 0.99$) (Fig. 6a). Fig. 6b shows the co-expression of F4/80 and HO-1. We found almost no HO-1 expression in F4/80-positive macrophages in the DSS group. Obviously, large numbers of F4/80-positive macrophages expressing HO-1 flood were found in the colonic mucosa of mice in the HEA and LEA groups compared with the DSS group (both $P < 0.001$).

4. Discussion

In our study, we proved that high-frequency (100 Hz) and low-frequency (10 Hz) EA at the ST36 acupoint could ameliorate colonic inflammation in mice with acute DSS-induced colitis. The beneficial effects of EA presented as a regulation of macrophage polarization and the suppression of NLRP3/IL-1β and promotion of Nrf2/HO-1 pathways.

EA, derived from acupuncture in traditional Chinese medicine, has been demonstrated to promote gastrointestinal motility in animal models (Chen et al., 2013; Iwa et al., 2006). However, the effect of EA on inflammatory bowel disease has not been confirmed. The beneficial effect of EA on 2,4,6-trinitrobenzene sulphonic acid (TNBS)-induced colitis rats and DSS-induced colitis mice has been demonstrated by decreased DAI scores and the remission of colonic histological features in a few previous studies (Goes et al., 2014; Jin et al., 2017; Sun et al., 2017; Wu et al., 2007). In the present study, we demonstrated that EA lowered DAI and histological scores, reduced the serum levels of pro-inflammatory cytokines, and decreased the colonic levels of IL-1β, TNFα and IL17. In addition, HEA was more effective at increasing IL-10 levels, suggesting that EA, especially the HEA, is effective in attenuating colitis through regulating inflammatory cytokines.

In recent years, macrophages have been found to be highly activated in the infiltration of colonic lamina propria, which contributes on the development and perpetuation of colonic inflammation (Gren and Grip, 2016; Mahida, 2000). M1 macrophages are characterized by high levels of pro-inflammatory cytokine expression and high levels of iNOS production, which promotes strong pro-inflammatory effects (Isidro and Appleyard, 2016). In contrast, M2 macrophages are able to resist inflammation and promote the healing of mucosal disruption with high expression levels of mannose receptors (CD206), resistin-likeα (FIZZ1) and Arg1 (Loke et al., 2002). Zhu et al showed that the percentage of M1 macrophages was increased, while the percentage of M2 macrophages was decreased during the development of acute DSS-induced

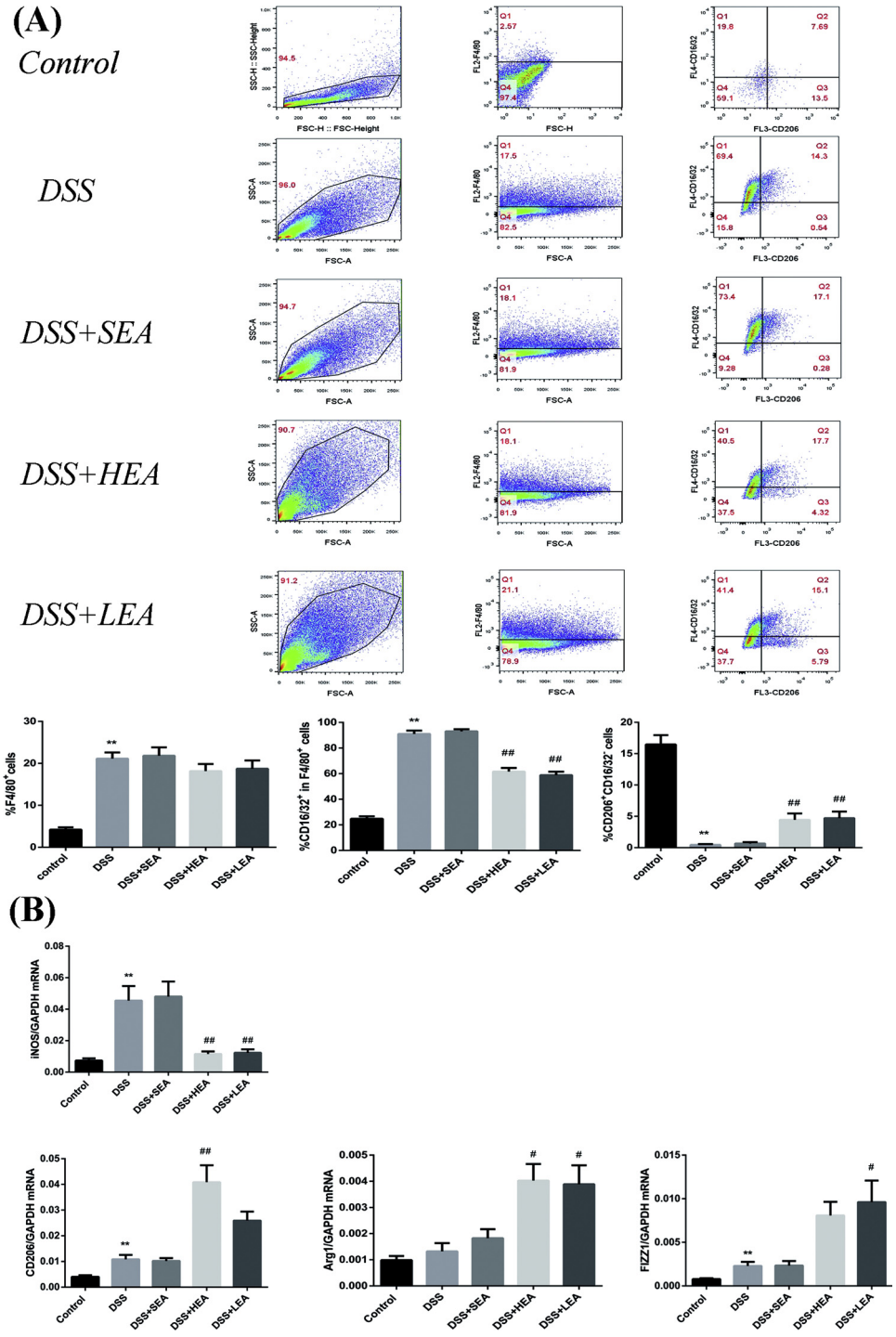

Fig. 4. EA decreased M1 macrophage activation and increased M2 macrophage activation following DSS exposure. (**A**) Representative flow cytometric analysis of lamina propria mononuclear cells. The percentages of total macrophages, M1 macrophages and M2 macrophages are shown, n = 4 in each group. (**B**) The mRNA expression of M1-associated genes (iNOS) and M2-associated genes (CD206, Arg1 and FIZZ1) in macrophages were examined by RT-PCR analysis, n = 4 in each group. $^{**}P < 0.01$ compared with the control group, $^{\#}P < 0.05$compared with the DSS group and $^{\#\#}P < 0.01$compared with the DSS group. Arg-1, arginase-1.

colitis; moreover, colitis was relieved after transferring M2 macrophages, whereas the opposite outcome was obtained with M1 macrophage transfer (Zhu et al., 2014). Hunter et al also discovered that the injection of M2 macrophages, but not M1 macrophages, significantly reduced the severity of dinitrobenzene sulfonic acid (DNBS)-induced colitis in mice. They also showed that the number $CD68^{+}CD206^{+}$ macrophages (which represent M2 macrophages) was reduced in patients with active Crohn's disease (CD) (Hunter et al., 2010). In addition, the application of M2 macrophage inducing factors was found to effectively ameliorate experimental colitis (Chang et al., 2013; Jang et al., 2013). Our previous research indicated that EA protected interstitial cells of Cajal via sustaining HO-1-positive M2 macrophages in the stomachs of diabetic mice (Tian et al., 2018). However, no study has investigated the effect of EA on macrophage subsets in an experimental model of colitis. In the current study, we discovered that both the HEA and LEA inhibited M1 macrophages while prompted M2 macrophages, indicating that maintaining an equilibrium between M1 and M2 macrophages may be one of the possible mechanisms by which EA

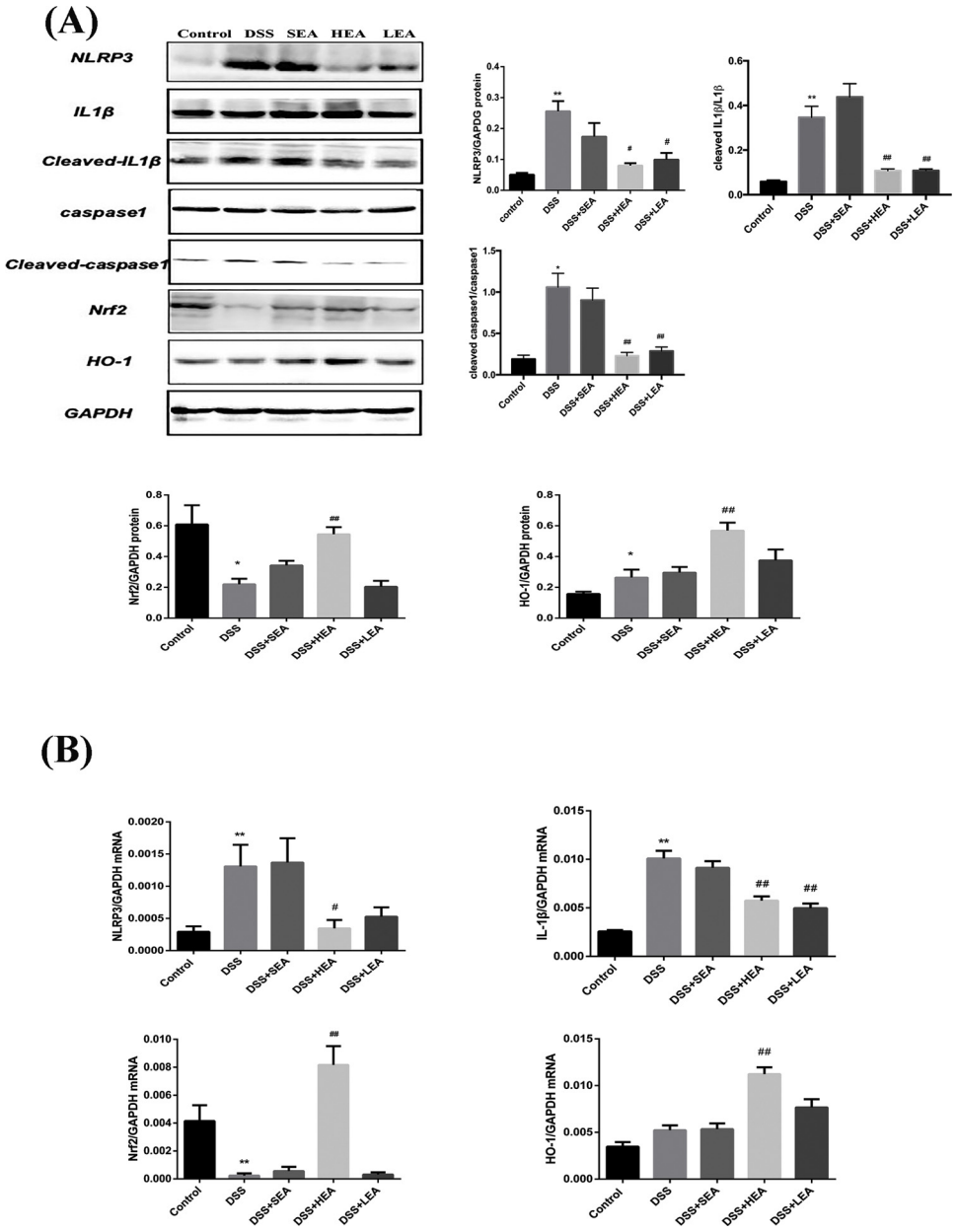

Fig. 5. EA suppress the activation of NLRP3/IL-1β and promotes Nrf2/HO-1 activation in macrophages compared with activity in the DSS group (**A**) The protein levels of NLRP3, caspase1, cleaved caspase, IL-1β, cleaved IL-1β, Nrf2 and HO-1 in macrophages were measured by western blotting analysis. n = 4 in each group. (**B**) The mRNA expression of NLRP3, IL-1β, Nrf2 and HO-1 in macrophages was examined by RT-PCR analysis. n = 4 in each group. $^{*}P < 0.05$ compared with the control group, $^{**}P < 0.01$ compared with the control group, $^{\#}P < 0.05$ compared with the control group and $^{\#\#}P < 0.01$ compared with the DSS group.

decreases the severity of acute DSS-induced colitis.

Finally, we explored the molecular mechanisms underlying how EA regulates macrophages in DSS-induced colitis. NLRP3 is the most extensively studied inflammasome; it is formed rapidly in macrophages responding to inflammatory stimulation and plays a significant role in developing acute colitis. Wu et al suggested that LPS-induced production of IL-1β was reduced by inhibiting NLRP3 activation in THP-1 cells and primary peritoneal macrophages (Wu et al., 2014). It was found the promotion of NLRP3 activation and IL-1β production in macrophages was crucial during the induction phase of acute colitis (Simovic Markovic et al., 2016). In addition, Fuente et al showed that *Escherichia coli*, which can survive in macrophages, may contribute to the pathogenesis of CD and UC as a result of IL-1β production through an NLRP3-dependent mechanism (De la Fuente et al., 2014). Furthermore, researchers concluded that the burst of colonic inflammatory responses in experimental colitis was attributed to failed post-transcriptional control of NLRP3 inflammasome activation in colonic macrophages (Filardy et al., 2016). In the current study, we demonstrated that HEA and LEA could inhibit NLRP3 and caspase1 activation in macrophages in the mice with acute DSS-induced colitis, following the level of cleaved-IL1β was reduced, suggesting that the suppression of the NLRP3/IL-1β pathway in macrophages may be involved in the anti-inflammatory effects of EA on colitis.

In addition, we discovered that HEA could promote Nrf2/HO-1 expression in macrophages relative to activity in the DSS group. Nrf2 is the key transcription factor that regulates the antioxidant response through the synthesis of HO-1. Some lines of evidence have revealed that the activation of Nrf2 protects mice against DSS-induced colitis (Lu et al., 2016; Wang et al., 2015). Moreover, several reports have described HO-1-overexpressing macrophages as having anti-inflammatory and cytoprotective abilities. Harusato et al proved that colonic macrophages with high expression of HO-1 inhibited TNBS-induced colitis

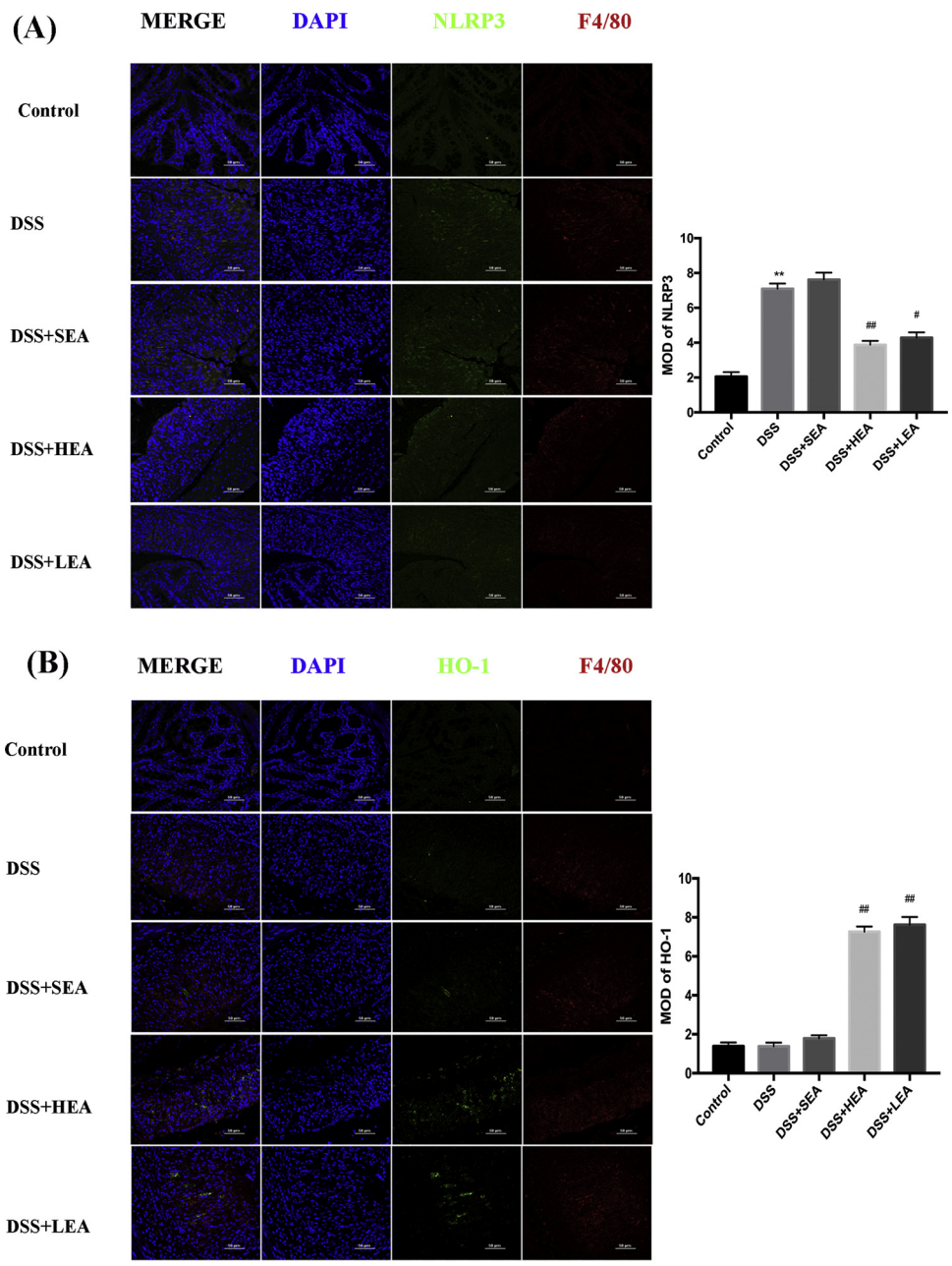

Fig. 6. EA inhibited NLRP3 activation and promoted HO-1 secretion in macrophages in colonic sections compared with activity in the DSS group. **(A)** Double-labelling with NLRP3 (green) and F4/80 (red), n = 6 in each group; **(B)** HO-1 (green) and F4/80 (red) in the different groups, n = 6 in each group. Nuclei were stained with DAPI (blue). HO-1, haeme oxygenase-1 (For interpretation of the references to colour in this figure legend, the reader is referred to the web version of this article).

(Harusato et al., 2013); and Sheikh et al discovered that the pharmacological induction of HO-1 resulted in an increased number of HO-1-positive and IL-10-positive macrophages, which play an anti-inflammatory effect in experimental colitis models (Sheikh et al., 2011). Furthermore, there is a positive feedback circuit between HO-1 and IL-10. HO-1 expression is related to IL-10 secretion and vice versa (Naito et al., 2014), which might amplify the anti-inflammatory effects of HO-1 in macrophages. According to our results, promoting the Nrf2/HO-1 pathway in macrophages may be one of the mechanisms underlying the benefits of HEA in DSS-induced colitis.

5. Conclusions

In summary, we provided evidence that EA at acupoint ST-36 could ameliorate acute DSS-induced colitis and illustrated a potential underlying mechanism: a decrease in the proportion of M1 macrophages and an increase in the proportion of M2 macrophages. The molecular mechanisms involved in EA attenuating colonic inflammation include the downregulation of NLRP3/IL-1β and upregulation of Nrf2/HO-1 pathways. Our study hints that EA might act as a safe and cost-effectiveness candidate therapy for acute colitis that could have advantages for potential clinical applications. However, UC is a chronic disease with a complicated clinical manifestation, and clinical trials studying the effects of EA on UC patients are scarce, so optimizing the parameters for EA and gaining a better understanding of its effects on different courses of chronic UC warrant further research and exploration.

Author contributions statements

SN-S and SL designed the experiment; SNS, JA and YL-L performed the experiments; SN-S analyzed the data; SN-S draft the manuscript; SL revised the manuscript and approved the final version of manuscript.

Funds

The work was supported by grants from the National Natural Science Foundation of China (grant numbers 81570488, 81770536).

Compliance with ethical standards

This studs involved in animals were carried out in accordance with the principles of the Guide for the Care and Use of Laboratory Animals of Tongji Medical College, the Committee of Experimental Animals of Tongji Medical College of Huazhong University of Science and Technology.

Declarations of interest

None.

References

Bang, B., Lichtenberger, L.M., 2016. Methods of inducing inflammatory bowel disease in mice. Curr. Protoc. Pharmacol. 72 (5), 1–42 58.

Bauer, C., Duewell, P., Mayer, C., Lehr, H.A., Fitzgerald, K.A., Dauer, M., Tschopp, J., Endres, S., Latz, E., Schnurr, M., 2010. Colitis induced in mice with dextran sulfate sodium (DSS) is mediated by the NLRP3 inflammasome. Gut 59, 1192–1199.

Chang, H.H., Miaw, S.C., Tseng, W., Sun, Y.W., Liu, C.C., Tsao, H.W., Ho, I.C., 2013. PTPN22 modulates macrophage polarization and susceptibility to dextran sulfate sodium-induced colitis. J. Immunol. 191, 2134–2143.

Chen, Y., Xu, J.J., Liu, S., Hou, X.H., 2013. Electroacupuncture at ST36 ameliorates gastric emptying and rescues networks of interstitial cells of Cajal in the stomach of diabetic rats. PLoS One 8, e83904.

De la Fuente, M., Franchi, L., Araya, D., Diaz-Jimenez, D., Olivares, M., Alvarez-Lobos, M., Golenbock, D., Gonzalez, M.J., Lopez-Kostner, F., Quera, R., Nunez, G., Vidal, R., Hermoso, M.A., 2014. Escherichia coli isolates from inflammatory bowel diseases patients survive in macrophages and activate NLRP3 inflammasome. Int. J. Med. Microbiol. 304, 384–392.

Filardy, A.A., He, J., Bennink, J., Yewdell, J., Kelsall, B.L., 2016. Posttranscriptional control of NLRP3 inflammasome activation in colonic macrophages. Mucosal Immunol. 9, 850–858.

Geremia, A., Biancheri, P., Allan, P., Corazza, G.R., Di Sabatino, A., 2014. Innate and adaptive immunity in inflammatory bowel disease. Autoimmun. Rev. 13, 3–10.

Goes, A.C., Pinto, F.M., Fernandes, G.C., Barbosa, J.S., Correia, E.S., Ribeiro, R.A., Guimaraes, S.B., Lima Junior, R.C., Brito, G.A., Rodrigues, L.V., 2014. Electroacupuncture ameliorates experimental colitis induced by TNBS through activation of interleukin-10 and inhibition of iNOS in mice. Acta Cir. Bras. 29, 787–793.

Gren, S.T., Grip, O., 2016. Role of monocytes and intestinal macrophages in Crohn's disease and ulcerative colitis. Inflamm. Bowel Dis. 22, 1992–1998.

Harusato, A., Naito, Y., Takagi, T., Uchiyama, K., Mizushima, K., Hirai, Y., Higashimura, Y., Katada, K., Handa, O., Ishikawa, T., Yagi, N., Kokura, S., Ichikawa, H., Muto, A., Igarashi, K., Yoshikawa, T., 2013. BTB and CNC homolog 1 (Bach1) deficiency ameliorates TNBS colitis in mice: role of M2 macrophages and heme oxygenase-1. Inflamm. Bowel Dis. 19, 740–753.

Hunter, M.M., Wang, A., Parhar, K.S., Johnston, M.J., Van Rooijen, N., Beck, P.L., McKay, D.M., 2010. In vitro-derived alternatively activated macrophages reduce colonic inflammation in mice. Gastroenterology 138, 1395–1405.

Isidro, R.A., Appleyard, C.B., 2016. Colonic macrophage polarization in homeostasis, inflammation, and cancer. Am. J. Physiol. Gastrointest. Liver Physiol. 311, G59–73.

Iwa, M., Matsushima, M., Nakade, Y., Pappas, T.N., Fujimiya, M., Takahashi, T., 2006. Electroacupuncture at ST-36 accelerates colonic motility and transit in freely moving conscious rats. Am. J. Physiol. Gastrointest. Liver Physiol. 290, G285–92.

Jang, S.E., Hyam, S.R., Han, M.J., Kim, S.Y., Lee, B.G., Kim, D.H., 2013. Lactobacillus brevis G-101 ameliorates colitis in mice by inhibiting NF-kappaB, MAPK and AKT pathways and by polarizing M1 macrophages to M2-like macrophages. J. Appl. Microbiol. 115, 888–896.

Jin, H., Guo, J., Liu, J., Lyu, B., Foreman, R.D., Yin, J., Shi, Z., Chen, J.D.Z., 2017. Anti-inflammatory effects and mechanisms of vagal nerve stimulation combined with electroacupuncture in a rodent model of TNBS-induced colitis. Am. J. Physiol. Gastrointest. Liver Physiol. 313, G192–G202.

Kim, J., Cha, Y.N., Surh, Y.J., 2010. A protective role of nuclear factor-erythroid 2-related factor-2 (Nrf2) in inflammatory disorders. Mutat. Res. 690, 12–23.

Liu, X., Zhou, W., Zhang, X., Lu, P., Du, Q., Tao, L., Ding, Y., Wang, Y., Hu, R., 2016. Dimethyl fumarate ameliorates dextran sulfate sodium-induced murine experimental colitis by activating Nrf2 and suppressing NLRP3 inflammasome activation. Biochem. Pharmacol. 112, 37–49.

Loke, P., Nair, M.G., Parkinson, J., Guiliano, D., Blaxter, M., Allen, J.E., 2002. IL-4 dependent alternatively-activated macrophages have a distinctive in vivo gene expression phenotype. BMC Immunol. 3, 7.

Lu, M.C., Ji, J.A., Jiang, Y.L., Chen, Z.Y., Yuan, Z.W., You, Q.D., Jiang, Z.Y., 2016. An inhibitor of the Keap1-Nrf2 protein-protein interaction protects NCM460 colonic cells and alleviates experimental colitis. Sci. Rep. 6, 26585.

Mahida, Y.R., 2000. The key role of macrophages in the immunopathogenesis of inflammatory bowel disease. Inflamm. Bowel Dis. 6, 21–33.

Naito, Y., Takagi, T., Higashimura, Y., 2014. Heme oxygenase-1 and anti-inflammatory M2 macrophages. Arch. Biochem. Biophys. 564, 83–88.

Ng, S.C., Bernstein, C.N., Vatn, M.H., Lakatos, P.L., Loftus, E.V., Tysk, C., O'Morain, C., Moum, B., Colombel, J.-F., 2013. Geographical variability and environmental risk factors in inflammatory bowel disease. Gut 62, 630–649.

Sheikh, S.Z., Hegazi, R.A., Kobayashi, T., Onyiah, J.C., Russo, S.M., Matsuoka, K., Sepulveda, A.R., Li, F., Otterbein, L.E., Plevy, S.E., 2011. An anti-inflammatory role for carbon monoxide and heme oxygenase-1 in chronic Th2-mediated murine colitis. J. Immunol. 186, 5506–5513.

Shouval, D.S., Biswas, A., Goettel, J.A., McCann, K., Conaway, E., Redhu, N.S., Mascanfroni, I.D., Al Adham, Z., Lavoie, S., Ibourk, M., Nguyen, D.D., Samsom, J.N., Escher, J.C., Somech, R., Weiss, B., Beier, R., Conklin, L.S., Ebens, C.L., Santos, F.G., Ferreira, A.R., Sherlock, M., Bhan, A.K., Muller, W., Mora, J.R., Quintana, F.J., Klein, C., Muise, A.M., Horwitz, B.H., Snapper, S.B., 2014. Interleukin-10 receptor signaling in innate immune cells regulates mucosal immune tolerance and anti-inflammatory macrophage function. Immunity 40, 706–719.

Simovic Markovic, B., Nikolic, A., Gazdic, M., Bojic, S., Vucicevic, L., Kosic, M., Mitrovic, S., Milosavljevic, M., Besra, G., Trajkovic, V., Arsenijevic, N., Lukic, M.L., Volarevic, V., 2016. Galectin-3 plays an important pro-inflammatory role in the induction phase of acute colitis by promoting activation of NLRP3 inflammasome and production of IL-1beta in macrophages. J. Crohns Colitis 10, 593–606.

Sun, J., Zhang, H., Wang, C., Yang, M., Chang, S., Geng, Y., Yang, H., Zhuang, Z., Wang, X., Xie, L., Huang, B., Zhao, N., Zhou, W., Cheng, X., Cai, B., Wu, Q., Yu, S.G., 2017. Regulating the balance of Th17/Treg via electroacupuncture and moxibustion: an ulcerative colitis mice model based study. Evid. Complement. Alternat. Med. 2017, 7296353.

Tian, L., Zhu, B., Liu, S., 2017. Electroacupuncture at ST36 protects ICC networks via mSCF/Kit-ETV1 signaling in the stomach of diabetic mice. Evid. Complement. Alternat. Med. 2017, 3980870.

Tian, L., Song, S., Zhu, B., Liu, S., 2018. Electroacupuncture at ST-36 protects interstitial cells of cajal via sustaining heme oxygenase-1 positive M2 macrophages in the stomach of diabetic mice. Oxid. Med. Cell. Longev. 2018, 3987134.

Wang, K.P., Zhang, C., Zhang, S.G., Liu, E.D., Dong, L., Kong, X.Z., Cao, P., Hu, C.P., Zhao, K., Zhan, Y.Q., Dong, X.M., Ge, C.H., Yu, M., Chen, H., Wang, L., Yang, X.M., Li, C.Y., 2015. 3-(3-pyridylmethylidene)-2-indolinone reduces the severity of colonic injury in a murine model of experimental colitis. Oxid. Med. Cell. Longev. 2015, 959253.

Wang, Y., Wang, H., Qian, C., Tang, J., Zhou, W., Liu, X., You, Q., Hu, R., 2016. 3-(2-Oxo-2-phenylethylidene)-2,3,6,7-tetrahydro-1H-pyrazino[2,1-a]isoquinolin-4(1 1bH)-one (compound 1), a novel potent Nrf2/ARE inducer, protects against DSS-induced colitis via inhibiting NLRP3 inflammasome. Biochem. Pharmacol. 101, 71–86.

Weigmann, B., Tubbe, I., Seidel, D., Nicolaev, A., Becker, C., Neurath, M.F., 2007. Isolation and subsequent analysis of murine lamina propria mononuclear cells from colonic tissue. Nat. Protoc. 2, 2307–2311.

Wirtz, S., Neufert, C., Weigmann, B., Neurath, M.F., 2007. Chemically induced mouse models of intestinal inflammation. Nat. Protoc. 2, 541–546.

Wu, H.G., Liu, H.R., Tan, L.Y., Gong, Y.J., Shi, Y., Zhao, T.P., Yi, Y., Yang, Y., 2007. Electroacupuncture and moxibustion promote neutrophil apoptosis and improve ulcerative colitis in rats. Dig. Dis. Sci. 52, 379–384.

Wu, X.F., Ouyang, Z.J., Feng, L.L., Chen, G., Guo, W.J., Shen, Y., Wu, X.D., Sun, Y., Xu, Q., 2014. Suppression of NF-kappaB signaling and NLRP3 inflammasome activation in macrophages is responsible for the amelioration of experimental murine colitis by the natural compound fraxinellone. Toxicol. Appl. Pharmacol. 281, 146–156.

Yang, H., Li, Y., Wu, W., Sun, Q., Zhang, Y., Zhao, W., Lv, H., Xia, Q., Hu, P., Li, H., Qian, J., 2014. The incidence of inflammatory bowel disease in Northern China: a prospective population-based study. PLoS One 9, e101296.

Zhao, J., Ng, S.C., Lei, Y., Yi, F., Li, J., Yu, L., Zou, K., Dan, Z., Dai, M., Ding, Y., Song, M., Mei, Q., Fang, X., Liu, H., Shi, Z., Zhou, R., Xia, M., Wu, Q., Xiong, Z., Zhu, W., Deng, L., Kamm, M.A., Xia, B., 2013. First prospective, population-based inflammatory bowel disease incidence study in mainland of China: the emergence of "western" disease. Inflamm. Bowel Dis. 19, 1839–1845.

Zhu, W., Yu, J., Nie, Y., Shi, X., Liu, Y., Li, F., Zhang, X.L., 2014. Disequilibrium of M1 and M2 macrophages correlates with the development of experimental inflammatory bowel diseases. Immunol. Invest. 43, 638–652.